

Effects of resonance weak decay and hadronic rescattering on the proton number fluctuations in Au+Au collisions at $\sqrt{s_{NN}} = 5$ GeV from a microscopic hadronic transport (JAM) model

Yu Zhang (张宇) , Shu He (何澍), Hui Liu (刘慧) , Zhenzhen Yang (杨贞贞), and Xiaofeng Luo (罗晓峰) *

*Key Laboratory of Quark & Lepton Physics (MOE), Institute of Particle Physics,
Central China Normal University, Wuhan 430079, China*



(Received 2 July 2019; revised manuscript received 15 January 2020; accepted 19 February 2020; published 16 March 2020)

Proton number fluctuation is sensitive observable to search for the QCD critical point in heavy-ion collisions. In this paper, we studied rapidity acceptance dependence of the proton cumulants and correlation functions in most central Au+Au collisions at $\sqrt{s_{NN}} = 5$ GeV from a microscopic hadronic transport model [the jet AA microscopic transportation model (JAM)]. At midrapidity, we found the effects of resonance weak decays and hadronic rescattering on the proton cumulants and correlation functions are small, but those effects get larger when further increasing the rapidity acceptance. On the other hand, we found the baryon number conservation is a dominant background effect on the rapidity acceptance dependence of proton number fluctuations. It leads to a strong suppression of cumulants and cumulant ratios as well as the negative proton correlation functions. We also studied those two effects on the energy dependence of cumulant ratios of net-proton distributions in most central Au+Au collisions at $\sqrt{s_{NN}} = 5$ –200 GeV from the JAM model. This paper can serve as a noncritical baseline for a future QCD critical point search in heavy-ion collisions at the high baryon density region.

DOI: [10.1103/PhysRevC.101.034909](https://doi.org/10.1103/PhysRevC.101.034909)

I. INTRODUCTION

Exploring the QCD phase structure is one of the main goals of heavy-ion collision experiments. It can be displayed in the QCD phase diagram, which is a two-dimensional $T - \mu_B$ plane. Lattice QCD calculations confirmed that the transition from quark-gluon plasma to a hadronic phase at the zero baryon chemical potential ($\mu_B = 0$) is a smooth crossover [1]. QCD-based models predict a first-order phase transition at large μ_B [2]. If both the crossover and the first-order transitions are true, there must be an end point of the first-order phase-transition boundary, which is the so-called QCD critical point. The experimental and/or theoretical confirmation of the QCD critical point would be a landmark in exploring the QCD phase structure.

Fluctuations of conserved charges, such as net-baryon (B), net-charge (Q), and net-strangeness (S), are sensitive probes to the QCD critical point and phase transition in heavy-ion collisions [3–7]. These observables have been extensively studied experimentally [8–10] and theoretically [11–32]. In the years 2010–2014, the Brookhaven National Laboratory Relativistic Heavy Ion Collider (RHIC) has finished the first phase of a beam energy scan and took data of Au+Au collisions at $\sqrt{s_{NN}} = 7.7, 11.5, 14.5, 19.6, 27, 39, 62.4, 200$ GeV. With those experimental data, the STAR Collaboration experiment has measured the higher-order fluctuations of net-proton, net-charge, and net-kaon multiplicity distributions [9,10,34–36].

As shown in Fig. 1, one of the most striking observations is the nonmonotonic energy dependence of the fourth-order cumulants ratio ($\kappa\sigma^2$) of the net-proton and proton number fluctuations in most central (0–5%) Au+Au collisions [36]. It was observed that the fourth-order net-proton fluctuation is close to unity above 39 GeV but deviates significantly below unity at 19.6 and 27 GeV, then, becomes above unity at lower energies. This nonmonotonic structure is predicted by models assuming the existence of a critical point [21,37–42]. This may suggest that the created system skims close by the critical point and received positive and/or negative contributions from critical fluctuations. On the other hand, the enhancement of $\kappa\sigma^2$ at low energies cannot be described by the ultrarelativistic quantum molecular dynamics (UrQMD) model [43,44], which does not contain the physics of the critical point. For second- and third-order net-proton cumulant ratios (C_3/C_2 and C_2/C_1), they show deviations below from the Poisson expectations [34] and are dominated by the contributions from baryon number conservation (BNC).

To extract the signature of critical fluctuations, it is crucial to understand the background contributions for proton number fluctuations in heavy-ion collisions. Some of the background contributions, such as baryon number conservations [45], acceptance and efficiency corrections [46–48], light nuclei formation [49], initial volume fluctuations, autocorrelation, and the effects of centrality selections [50–53], have been studied before. However, these studied background effects have difficulties to describe the $\kappa\sigma^2 \gg 1$ at low energies. A phenomenological model study shows that the large increase in net-proton $\kappa\sigma^2$ above unity at $\sqrt{s_{NN}} = 7.7$ GeV can be explained as the formation of multiproton clusters [54,55].

* xfluo@mail.ccnu.edu.cn

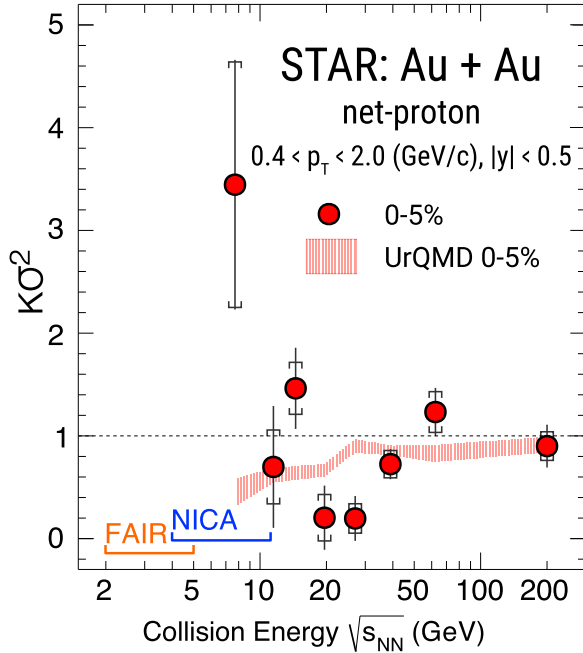


FIG. 1. Energy dependence of fourth-order cumulants ratio ($\kappa\sigma^2$) of net-proton multiplicity distributions from the STAR Collaboration experiment [33]. The energy coverage of the FAIR and NICA heavy-ion programs are marked as orange and blue caps in the plot, respectively.

One may note that, in Refs. [54,55], the n th-order cumulants and correlation functions are denoted as κ_n and C_n , respectively, which is opposite from what we used in the current paper.

In this paper, we performed detailed studies for the effects of resonance weak decays and hadronic rescattering on the proton number fluctuations in most central Au+Au collisions $\sqrt{s_{NN}} = 5$ GeV with the jet AA microscopic transportation model (JAM). The energy is chosen because it will be covered by the future CBM experiment at FAIR and MPD experiment at NICA. The resonance weak decays and hadronic rescattering can be turned on or off in the JAM model. For hadronic rescattering, we studied two effects: One is the effect of meson-baryon (MB) and meson-meson (MM) interactions, and the other is the hadronic elastic scattering. Finally, we show the energy dependence of net-proton cumulant ratios in most central Au+Au collisions at $\sqrt{s_{NN}} = 5$ –200 GeV from the JAM model.

This paper is organized as follows, we first introduce the fluctuation observables: cumulants and correlation functions in Sec. II. Then, we introduce the JAM model in Sec. III. In Sec. IV, we present the results of proton cumulants and correlation functions and discuss the effects of resonance weak decays and hadronic rescattering. Finally, we give a summary.

II. CUMULANTS AND CORRELATION FUNCTIONS

To characterize the multiplicity fluctuations, one can measure the cumulants of the particle multiplicity distributions.

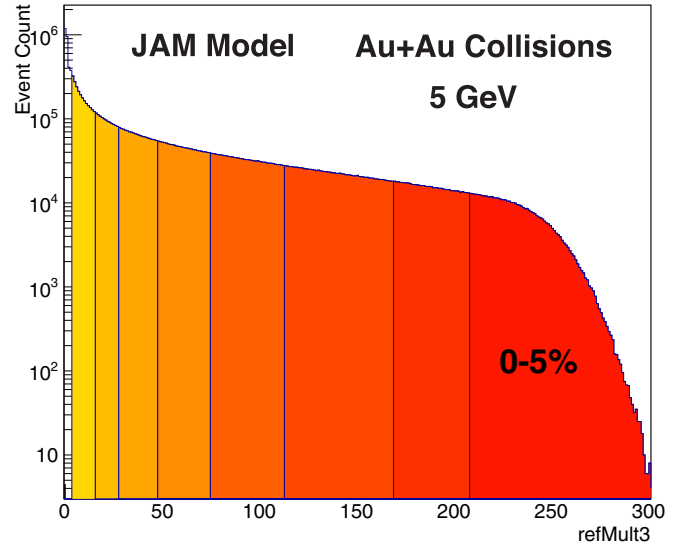


FIG. 2. The refMult3 distributions in Au+Au collisions at $\sqrt{s_{NN}} = 5$ GeV from the JAM model. It is defined as the number of charged (anti)pions and (anti)kaons within $|\eta| < 1$. Protons and antiprotons are excluded from this definition to avoid autocorrelation effects. Events from the top 5% centrality class are used in this analysis.

The various order cumulants are calculated from moments as

$$\begin{aligned}
 C_1 &= \langle N \rangle, \\
 C_2 &= \langle N^2 \rangle - \langle N \rangle^2, \\
 C_3 &= 2\langle N \rangle^3 - 3\langle N \rangle \langle N^2 \rangle + \langle N^3 \rangle, \\
 C_4 &= -6\langle N \rangle^4 + 12\langle N \rangle^2 \langle N^2 \rangle - 3\langle N^2 \rangle^2, \\
 &\quad - 4\langle N \rangle \langle N^3 \rangle + \langle N^4 \rangle,
 \end{aligned} \tag{1}$$

where $\langle N^n \rangle$ is the n th-order moment of the particle number distributions. The n th-order cumulant C_n is connected to the susceptibilities χ_n of the system as [56]

$$C_n = VT^3 \chi_n. \tag{2}$$

To cancel out the volume V , the ratios of different order of cumulants are usually constructed as experimental observables,

$$S\sigma = \frac{C_3}{C_2} = \frac{\chi_3}{\chi_2}, \quad \kappa\sigma^2 = \frac{C_4}{C_2} = \frac{\chi_4}{\chi_2}, \tag{3}$$

where S and κ are skewness and kurtosis of the multiplicity distributions, respectively.

The collision centralities are defined by using charged pions and kaons at midrapidity ($|\eta| < 1$), which is the so-called refMult3. In our paper as shown in Fig. 2, only the top 5% centrality is used in the calculations. The centrality bin width correction (CBWC) [50,57] is also applied to suppress volume fluctuations in a wide centrality bin. In the CBWC method as shown in Eq. (5), the cumulants are calculated for event ensembles in each refMult3 bin (i) and are taken an average with number of events (n_i) as the weights

TABLE I. Simulation options used to study the effects of resonance weak decays and hadronic rescattering. The data “MB and MM off” means that we disable meson-baryon and meson-meson interactions and only keep the baryon-baryon interactions. The “Elas. off” is to disable hadronic elastic scattering and to keep only inelastic scattering.

Identifier	Resonance weak decays	MB and MM scatterings	Elastic scattering
Full calculation	Yes	Yes	Yes
Decays off	No	Yes	Yes
MB and MM off	Yes	No	Yes
Elas. off	Yes	Yes	No
Decays and Elas. off	No	Yes	No

for each bin,

$$C_r = \frac{\sum n_i C_r^i}{\sum n_i}. \quad (4)$$

The Delta theorem is usually used to evaluate statistical uncertainties of the cumulants and cumulant ratios [47,58].

On the other hand, one can express the multiparticle correlation functions (also known as factorial cumulants) in terms of various order single-particle cumulants (i.e., proton cumulants but not net-proton cumulants) [54,59,60],

$$\begin{aligned} \kappa_2 &= -\langle N \rangle + C_2, \\ \kappa_3 &= 2\langle N \rangle - 3C_2 + C_3, \\ \kappa_4 &= -6\langle N \rangle + 11C_2 - 6C_3 + C_4. \end{aligned} \quad (5)$$

Thus, we also have

$$\begin{aligned} C_2 &= \langle N \rangle + \kappa_2, \\ C_3 &= \langle N \rangle + 3\kappa_2 + \kappa_3, \\ C_4 &= \langle N \rangle + 7\kappa_2 + 6\kappa_3 + \kappa_4, \end{aligned} \quad (6)$$

where the κ_n are used to denote various order correlation functions (or factorial cumulants). The κ_n ($n > 2$) of Poisson distributions are always zero. Thus, one can measure non-Poisson fluctuations from correlation functions. The correlation functions can be calculated by factorial moments F_n as

$$F_n = \langle N^n \rangle_f \equiv \langle N(N-1)\cdots(N-n+1) \rangle. \quad (7)$$

The relations between factorial moments and correlation functions are equivalent to those between moments and cumulants. Comparing with Eq. (2), we have

$$\begin{aligned} \kappa_2 &= F_2 - F_1^2, \\ \kappa_3 &= 2F_1^3 - 3F_1F_2 + F_3. \end{aligned} \quad (8)$$

It was predicted that the critical fluctuations can be encoded in the acceptance dependence of cumulants and/or correlation functions [59,61]. We found that the enhancement of $\kappa\sigma^2$ at 7.7 GeV in most central Au+Au collisions observed by the STAR Collaboration experiments is mainly due to the four-particle correlation function [54]. In our previous study with the UrQMD model [62], we observed large deviations

from experimental results in second- and fourth-order correlation functions. Thus, it is important to study the correlation functions to understand different noncritical contributions.

III. THE JAM MODEL

JAM is a simulation program which is designed to simulate relativistic nuclear collisions from the initial stage of nuclear collision to the final-state interaction in a hadronic gas state. In the JAM model, hadrons and their excited states have explicit space and time-evolution trajectories by the cascade method. Inelastic hadron-hadron collisions are modeled with resonance at low energy, string pictures at intermediate energy, and hard parton-parton scattering at high energy. In the JAM model, the nuclear mean field is implemented based on the simplified version of the relativistic quantum molecular dynamics approach. It is a skyrme-type density-dependent and Lorentzian-type momentum-dependent scalar mean-field potential [63]. More features can be seen in Refs. [64–67]. In the JAM model, one can study the effects of various types of equation of state (EoS).

Generally, the EoS of the medium can be expressed in the relation between the pressure and the energy density of the system: $p = p(\epsilon)$. The pressure of the system can be given by a virial theorem [68],

$$P = P_f + \Delta P, \quad (9)$$

where P_f is the free stream part and ΔP is determined by the momentum transfer in the two-body collision. ΔP can be reduced by introducing an attractive scattering angle, whereas it is increased by selecting a repulsive scattering orbit. In the JAM model, the attractive scattering orbit is used to simulate the effect of softening of the EoS for the first-order phase transition. For a cascade mode, the azimuthal angle of the two-body collision is chosen randomly. It means we select attractive or repulsive orbit of equal chance, which leads to the free hadron gas EoS. In the mean-field mode, nucleons feel repulsive interactions with other particles. Therefore, the ΔP in Eq. (9) is enhanced, and we get a stiffer EoS. In this paper, we use mean-field mode with parameters shown in Table I. The results from the attractive orbit and mean-field modes are compared with the results from the default cascade mode, separately. To study the effects of resonance weak decays and hadronic rescattering, we have produced five types of JAM model data with mean-field EoS, which is shown in Table I.

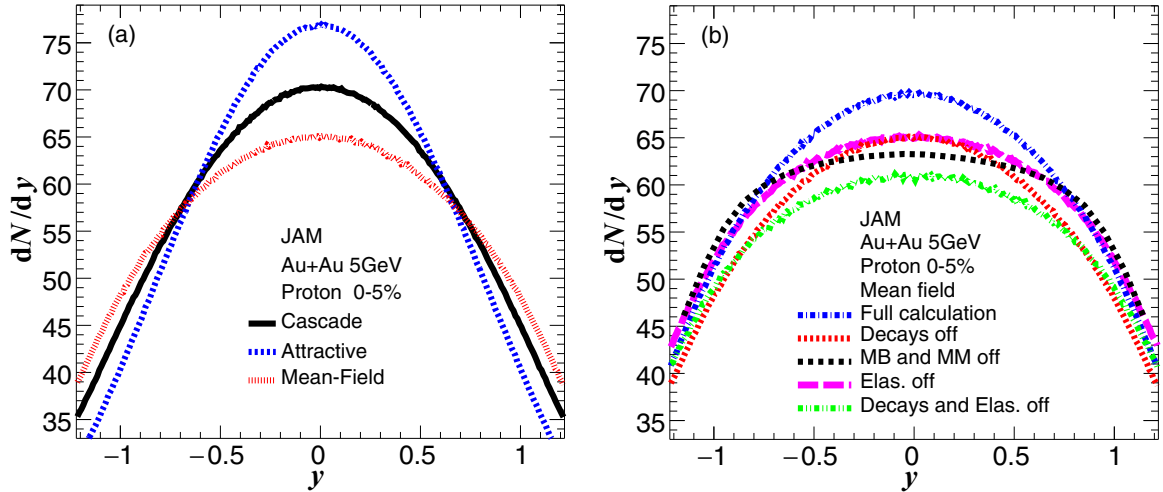


FIG. 3. Rapidity (dN/dy) distributions for proton in most central (0–5%) Au+Au collisions at $\sqrt{s_{NN}} = 5$ GeV. (a) Different EoS implemented in the JAM model (cascade, attractive rescattering orbit, and mean field). (b) dN/dy distributions with and without weak decays, MB and MM scatterings, and elastic scattering.

IV. RESULTS

A. Proton dN/dy and event-by-event distributions

In this section, we will discuss the proton dN/dy and the event-by-event proton number distributions in 0–5% most central Au+Au collisions at $\sqrt{s_{NN}} = 5$ GeV from different cases. Figure 3(a) shows the proton dN/dy distributions from three types of EoS. By comparing the distributions from different EoS, we found more protons are stopped at midrapidity due to the softening of EoS realized by using the attractive orbit scattering. However, due to the repulsive interactions, a lower mean value of the dN/dy distribution is observed for the mean-field mode.

In Fig. 3(b), we compared the proton dN/dy distributions from resonance weak decays and hadronic rescattering. It was observed that the proton dN/dy distributions show a

significant decrease when the weak decays switched off in the JAM model. On the other hand, the effects of hadronic rescattering are studied via disabling the MB and MM interactions and the elastic scattering among hadrons. We found the dN/dy distributions from the two cases become flatter and wider than the distribution from the full calculation. This is due to the reduced baryon stopping caused by switching off the MB and MM interactions and/or elastic rescattering. In the case of switching off the MB and MM interactions, only the baryon-baryon interactions and corresponding string excitation-fragmentation are playing a decisive role during the heavy-ion collision process.

Before discussing the results of proton cumulants and correlation functions, we show the event-by-event proton number distributions for different cases in 0–5% most central Au+Au collisions at $\sqrt{s_{NN}} = 5$ GeV. Figure 4(a) shows event-by-

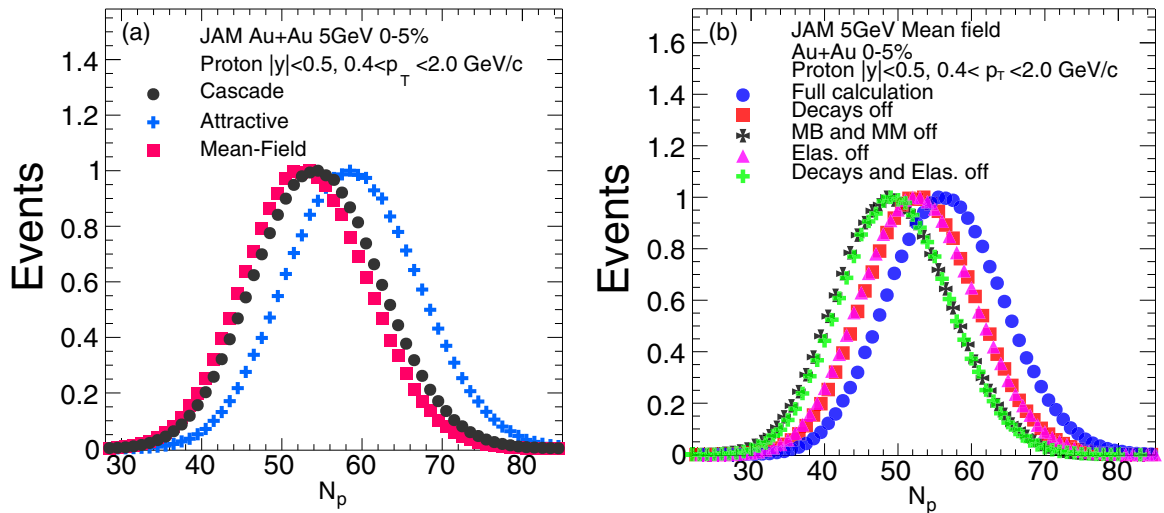


FIG. 4. Normalized event-by-event proton multiplicity distributions in most central (0–5%) Au+Au collisions at $\sqrt{s_{NN}} = 5$ GeV. N_p represents the proton number in an event. (a) Different EoS implemented in the JAM model (cascade, attractive rescattering orbit, and mean field). (b) With and without weak decays, MB and MM scatterings, and elastic scattering.

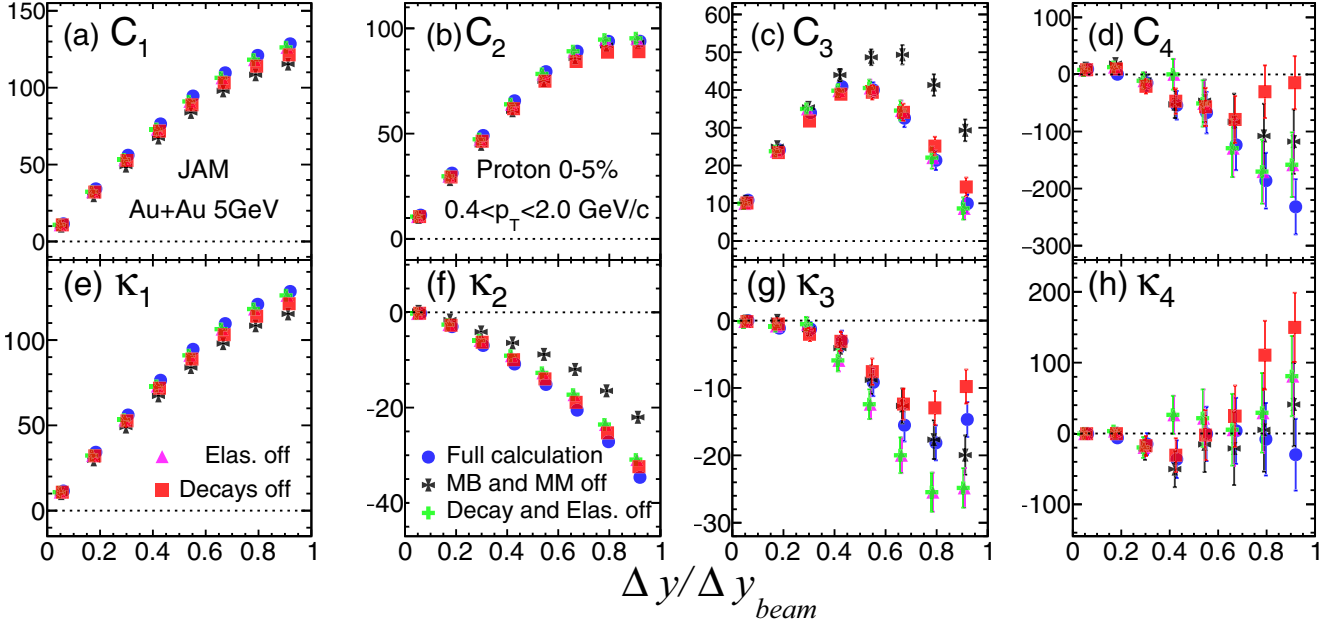


FIG. 5. Rapidity acceptance dependence of proton cumulants (C_1 – C_4) and correlation functions (κ_1 – κ_4) in 0–5% most central Au+Au collisions $\sqrt{s_{NN}} = 5$ GeV. The results are obtained with and without weak decays, MB and MM scatterings, and elastic scattering from the JAM model. In the x -axis label, $\Delta y = 2y'$ denotes $|y| < y'$ in calculations, and $y_{beam} = 1.63$ ($\Delta y_{beam} = 3.26$) is the beam rapidity for $\sqrt{s_{NN}} = 5$ GeV.

event proton number distributions for different EoS. We observed that a softer EoS (attractive scattering orbit) tends to have more protons stopped at midrapidity and the proton number distribution has a larger mean value than the results from cascade mode, whereas a stiffer EoS (mean field or repulsive potential) leads to a smaller mean value [69]. In Fig. 4(b), it is shown that the effects of weak decays can enhance the proton multiplicities at the midrapidity region similar to switching on MB and MM scatterings or elastic scattering. In Ref. [69], we concluded that the effects of mean-field (only include scalar interactions) and attractive rescattering orbits on proton number fluctuations are not significant and cannot lead to large proton C_4 or $\kappa\sigma^2$ at low energies. This might indicate the current JAM model does not capture the essential physics or true EoS that dominated the large increase in proton fourth-order cumulant C_4 . For example, currently, only the momentum dependence scalar potential is included in the mean field, but the vector potential could be also important. For future work, it would be interesting to study the mean-field effects by including both the scalar and the vector potentials. More importantly, there is no physics of phase transition and critical point implemented in the JAM model.

In the following, we focus on discussing the effects of resonance weak decays and hadronic rescattering on proton number fluctuations.

B. Rapidity acceptance dependence of proton cumulants and correlation functions

Theoretically, it was predicted that the rapidity acceptance dependence of the proton cumulants and correlation functions

are important observables to search for the QCD critical point and understand the smearing or nonequilibrium effects of dynamical expansion on the fluctuations in heavy-ion collisions [19,54,55,59,70,71]. Due to the long-range correlations near the critical point, it is expected that the proton cumulants (C_n) and/or multiproton correlation functions (κ_n) will be dominated by critical behavior, which shows power-law dependence as a function of number of protons and/or rapidity acceptance as $C_n, \kappa_n \propto (N_p)^n \propto (\Delta y)^n$ [59]. This requires the typical correlation length of the system near the critical point is larger than the rapidity interval ($\Delta y < \xi$). If the rapidity acceptance is further enlarged, and Δy becomes much larger than ξ ($\Delta y \gg \xi$), the proton cumulants and/or multiproton correlation functions will then be dominated by statistical fluctuations, which results in $C_n, \kappa_n \propto N_p \propto \Delta y$. However, the rapidity acceptance of the proton cumulants and multiproton correlation functions are also sensitive to the background effects, such as BNC. Thus, by comparing the acceptance dependence of proton cumulants and multiproton correlation from various simulation options from the JAM model, we can clearly demonstrate effects of BNC and other background effects, such as the equation of states, resonance weak decays, and hadronic rescattering effects.

Figure 5 shows rapidity acceptance dependence of various orders of proton cumulants and correlation functions in 0–5% most central Au+Au collisions at $\sqrt{s_{NN}} = 5$ GeV. We observed that the effects of resonance weak decays and hadronic rescattering on proton cumulants and correlation functions are small at midrapidity ($\Delta y/\Delta y_{beam} < 0.3$), but those effects get larger when further increasing the rapidity coverage. By making comparisons between results from different cases, we found the C_1 and C_2 values from full calculations are larger

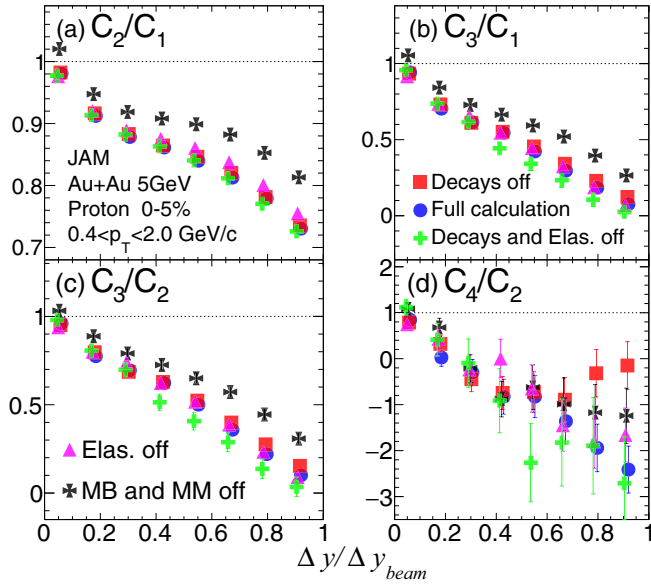


FIG. 6. Rapidity acceptance dependence of cumulant ratios of proton multiplicity distributions in the 0–5% most central Au+Au collisions at $\sqrt{s_{NN}} = 5$ GeV from the JAM model. To study the effects of weak decays and hadronic rescattering, we compared the results from five different types of the data generated by the JAM model.

than the other cases. This is mainly due to the resonance weak decays effects, especially the feed-down contributions of protons from Λ and Σ^+ . At the forward rapidity region, $\Delta y/\Delta y_{beam} > 0.4$, the MB and MM scatterings substantially suppress the C_3 values, whereas resonance weak decays and elastic scattering have very small effects on C_3 . For C_4 , the results of the different cases are consistent within statistical uncertainty. In addition, due to the baryon number conservation, the third- and fourth-order proton cumulants show strong suppression when increasing the rapidity acceptance as the effect of BNC becomes stronger when the fraction of proton number over total baryon in the acceptance gets larger [45]. In the second row of Fig. 5, we show various order proton correlation functions (κ_1 – κ_4) in 0–5% most central Au+Au collisions at $\sqrt{s_{NN}} = 5$ GeV from different cases. At midrapidity, we find that the effects of resonance weak decays and hadronic elastic scattering on the various order proton correlation functions are small. The resonance weak decays and hadronic rescattering slightly suppress the two-proton correlation function κ_2 . Due to BNC, the κ_2 is negative and monotonically decreases when enlarging the rapidity acceptance. This is because the BNC leads to anticorrelation of protons separated by any rapidity intervals. However, κ_3 and κ_4 are almost flat and close to zero at midrapidity ($\Delta y/\Delta y_{beam} < 0.3$), which means that the higher-order ($n > 2$) correlation functions are less sensitive to the effect of BNC. Furthermore, the MB and MM scatterings lead to larger suppression of the two-particle correlation functions κ_2 than the results from the case by turning them off.

In Fig. 6, we show the rapidity acceptance dependence of various order proton cumulant ratios in 0–5% most central

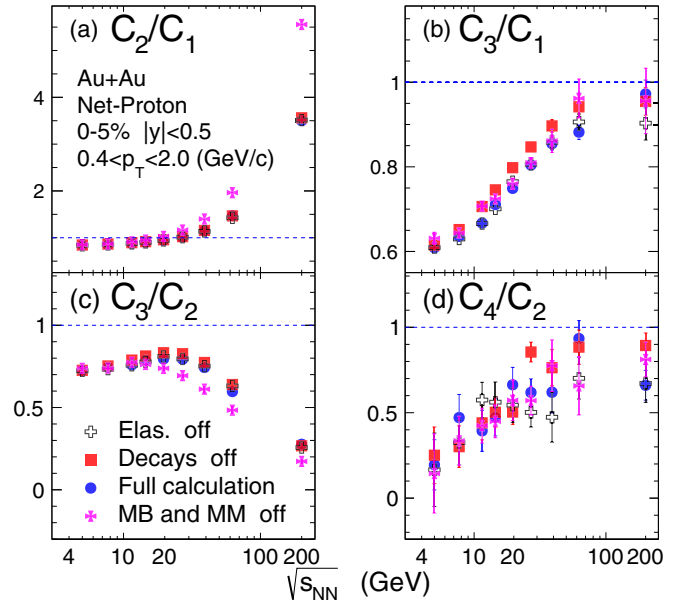


FIG. 7. Energy dependence of cumulant ratios of net-proton multiplicity distributions in 0–5% most central Au+Au collisions at $\sqrt{s_{NN}} = 5, 7.7, 11.5, 14.5, 19.6, 27, 39, 62.4, 200$ GeV from the JAM model. To study the effects of weak decays and hadronic rescattering, we compared the results from four different types of the data generated from the JAM model.

Au+Au collisions at $\sqrt{s_{NN}} = 5$ GeV. Generally, the proton cumulant ratios decrease when increasing the rapidity acceptance. This can be explained by the effects of BNC. The hadronic rescattering via turning on MB and MM scatterings suppress the second- and third-order cumulant ratios (C_2/C_1 , C_3/C_1 , and C_3/C_2). However, the resonance weak decays and elastic scattering have little influence on these cumulant ratios.

C. Energy dependence of net-proton cumulant ratios

As shown Fig. 1, nonmonotonic energy dependence of fourth-order fluctuations $\kappa\sigma^2$ of the net-proton multiplicity distribution is observed in the RHIC beam energy scan program. This observation is consistent with the theoretical expectations by assuming the presence of the QCD critical point. However, one needs to study the background contributions to the observable carefully, especially to understand how those backgrounds depend on the collision energies. In this paper, we focus on discussing the effects of resonance weak decay and hadronic rescattering. Figure 7 shows energy dependence of net-proton cumulant ratios in 0–5% most central Au+Au collisions with four different cases. We found that the effects of hadronic elastic scattering on various order net-proton cumulant ratios are not significant. However, by switching off the MB and MM collisions, we observed the cumulant ratios C_3/C_2 are suppressed whereas the cumulant ratios C_2/C_1 are significantly enhanced, especially at high energy. On the other hand, the effects of resonance weak decays suppress the third-order cumulant ratios (C_3/C_1 and C_3/C_2). For C_4/C_2 , it shows a monotonic decreasing trend when decreasing the collision

energy, and the results from four different cases are consistent within statistical uncertainties. The C_4/C_2 values are below Poisson baseline (unity) and cannot describe the nonmonotonic energy dependence trend of $\kappa\sigma^2$ in most central Au+Au collisions observed in the STAR Collaboration data.

As discussed in Ref. [69], the JAM model used in this analysis only includes the momentum dependence scalar potential in the mean field and does not implement the physics of the critical point and phase transition. It would be interesting to study those effects on the proton number fluctuations in the future.

V. SUMMARY

We studied the effects of resonance weak decays and hadronic re-scattering on proton cumulants and correlation functions in Au+Au collisions at $\sqrt{s_{NN}} = 5$ GeV within the JAM model. For the hadronic rescattering, we further studied the effects of MB and MM interactions and elastic hadronic scattering. In general, at the midrapidity region, the effects of resonance weak decays and hadronic rescattering on proton cumulants and correlation functions are small, but those effects get larger when further increasing the rapidity acceptance. The weak decays and hadronic rescattering enhance the mean values and width of the proton number distributions at midrapidity Au+Au collisions, whereas those two effects slightly suppress the two-particle correlation functions of protons. The MB and MM scatterings suppress the second- and third-order cumulant ratios (C_2/C_1 , C_3/C_1 , and C_3/C_2). On the other hand, the baryon number conservation is a dominant

background effect on the rapidity acceptance dependence of proton number fluctuations. It leads to a strong suppression of cumulants and cumulant ratios as well as the negative proton correlation functions. However, the higher-order correlation functions are less sensitive to the BNC. We also discussed the energy dependence of various order net-proton cumulant ratios in 0–5% most central Au+Au collisions at $\sqrt{s_{NN}} = 5$ –200 GeV. We found that the effects of hadronic elastic scattering on various order net-proton cumulant ratios are not significant within statistical uncertainties and the resonance weak decays suppress the third-order cumulant ratios (C_3/C_1 and C_3/C_2). The effects of switching off the MB and MM interactions significantly suppress the values of C_3/C_2 and enhance the values of C_2/C_1 especially at high energy. Due to the effect of BNC, the values of $\kappa\sigma^2$ (C_4/C_2) are significantly below the Poisson baseline (unity) at low energies and cannot describe the nonmonotonic energy dependence trend in most central Au+Au collisions observed in the STAR Collaboration data. Our paper provides useful noncritical baselines for the future QCD critical point search in heavy-ion collisions at the high baryon density region.

ACKNOWLEDGMENTS

We thank Dr. N. Xu for a stimulating discussion. This work was supported by the National Key Research and Development Program of China (Grant No. 2018YFE0205201), the National Natural Science Foundation of China (Grants No.11828501, No. 11575069, No. 11890711, and No. 11861131009).

-
- [1] Y. Aoki, G. Endrodi, Z. Fodor, S. D. Katz, and K. K. Szabo, *Nature (London)* **443**, 675 (2006).
 - [2] S. Ejiri, *Phys. Rev. D* **78**, 074507 (2008).
 - [3] S. Ejiri, F. Karsch, and K. Redlich, *Phys. Lett. B* **633**, 275 (2006).
 - [4] M. A. Stephanov, *Phys. Rev. Lett.* **102**, 032301 (2009).
 - [5] M. A. Stephanov, *Phys. Rev. Lett.* **107**, 052301 (2011).
 - [6] B. J. Schaefer and M. Wagner, *Phys. Rev. D* **85**, 034027 (2012).
 - [7] M. Asakawa, S. Ejiri, and M. Kitazawa, *Phys. Rev. Lett.* **103**, 262301 (2009).
 - [8] M. M. Aggarwal *et al.* (STAR Collaboration), *Phys. Rev. Lett.* **105**, 022302 (2010).
 - [9] L. Adamczyk *et al.* (STAR Collaboration), *Phys. Rev. Lett.* **113**, 092301 (2014).
 - [10] L. Adamczyk *et al.* (STAR Collaboration), *Phys. Rev. Lett.* **112**, 032302 (2014).
 - [11] F. Karsch and K. Redlich, *Phys. Lett. B* **695**, 136 (2011).
 - [12] P. Braun-Munzinger, B. Friman, F. Karsch, K. Redlich, and V. Skokov, *Phys. Rev. C* **84**, 064911 (2011).
 - [13] R. V. Gavai and S. Gupta, *Phys. Lett. B* **696**, 459 (2011).
 - [14] J.-W. Chen, J. Deng, and L. Labun, *Phys. Rev. D* **92**, 054019 (2015).
 - [15] J.-W. Chen, J. Deng, H. Kohyama, and L. Labun, *Phys. Rev. D* **93**, 034037 (2016).
 - [16] M. Kitazawa and M. Asakawa, *Phys. Rev. C* **85**, 021901(R) (2012).
 - [17] M. Kitazawa and M. Asakawa, *Phys. Rev. C* **86**, 024904 (2012); **86**, 069902(E) (2012).
 - [18] B. Friman, F. Karsch, K. Redlich, and V. Skokov, *Eur. Phys. J. C* **71**, 1694 (2011).
 - [19] S. Mukherjee, R. Venugopalan, and Y. Yin, *Phys. Rev. C* **92**, 034912 (2015).
 - [20] S. Mukherjee, R. Venugopalan, and Y. Yin, *Phys. Rev. Lett.* **117**, 222301 (2016).
 - [21] V. Vovchenko, D. V. Anchishkin, M. I. Gorenstein, and R. V. Poberezhnyuk, *Phys. Rev. C* **92**, 054901 (2015).
 - [22] L. Jiang, P. Li, and H. Song, *Phys. Rev. C* **94**, 024918 (2016).
 - [23] M. Nahrgang, M. Bluhm, P. Alba, R. Bellwied, and C. Ratti, *Eur. Phys. J. C* **75**, 573 (2015).
 - [24] K. Morita, B. Friman, and K. Redlich, *Phys. Lett. B* **741**, 178 (2015).
 - [25] A. Bazavov *et al.*, *Phys. Rev. Lett.* **109**, 192302 (2012).
 - [26] S. Borsanyi, Z. Fodor, S. D. Katz, S. Krieg, C. Ratti, and K. K. Szabo, *Phys. Rev. Lett.* **111**, 062005 (2013).
 - [27] P. Alba, W. Alberico, R. Bellwied, M. Bluhm, V. Mantovani Sarti, M. Nahrgang, and C. Ratti, *Phys. Lett. B* **738**, 305 (2014).
 - [28] W. Fan, X. Luo, and H.-S. Zong, *Int. J. Mod. Phys. A* **32**, 1750061 (2017).
 - [29] W. Fan, X. Luo, and H. Zong, *Chin. Phys. C* **43**, 054109 (2019).
 - [30] W. Fan, X. Luo, and H. Zong, *Chin. Phys. C* **43**, 033103 (2019).
 - [31] Z. Li, K. Xu, X. Wang, and M. Huang, *Eur. Phys. J. C* **79**, 245 (2019).

- [32] Y. Ye, Y. Wang, J. Steinheimer, Y. Nara, H.-j. Xu, P. Li, D. Lu, Q. Li, and H. Stoecker, *Phys. Rev. C* **98**, 054620 (2018).
- [33] J. Adam *et al.* (STAR Collaboration), [arXiv:2001.02852](https://arxiv.org/abs/2001.02852) [nucl-ex].
- [34] X. Luo, *Nucl. Phys. A* **956**, 75 (2016).
- [35] L. Adamczyk *et al.* (STAR Collaboration), *Phys. Lett. B* **785**, 551 (2018).
- [36] X. Luo and N. Xu, *Nucl. Sci. Tech.* **28**, 112 (2017).
- [37] M. A. Stephanov, *J. Phys. G: Nucl. Part. Phys.* **38**, 124147 (2011).
- [38] M. Bluhm, M. Nahrgang, S. A. Bass, and T. Schaefer, *Eur. Phys. J. C* **77**, 210 (2017).
- [39] M. Bluhm, M. Nahrgang, S. A. Bass, and T. Schäfer, *J. Phys.: Conf. Ser.* **779**, 012074 (2017).
- [40] C. Herold, M. Nahrgang, Y. Yan, and C. Kobdaj, *Phys. Rev. C* **93**, 021902(R) (2016).
- [41] A. Mukherjee, J. Steinheimer, and S. Schramm, *Phys. Rev. C* **96**, 025205 (2017).
- [42] M. Nahrgang and C. Herold, *Eur. Phys. J. A* **52**, 240 (2016).
- [43] J. Xu, S. Yu, F. Liu, and X. Luo, *Phys. Rev. C* **94**, 024901 (2016).
- [44] C. Zhou, J. Xu, X. Luo, and F. Liu, *Phys. Rev. C* **96**, 014909 (2017).
- [45] A. Bzdak, V. Koch, and V. Skokov, *Phys. Rev. C* **87**, 014901 (2013).
- [46] A. Bzdak and V. Koch, *Phys. Rev. C* **86**, 044904 (2012).
- [47] X. Luo, *Phys. Rev. C* **91**, 034907 (2015).
- [48] X. Luo and T. Nonaka, *Phys. Rev. C* **99**, 044917 (2019).
- [49] Z. Fecková, J. Steinheimer, B. Tomášik, and M. Bleicher, *Phys. Rev. C* **92**, 064908 (2015).
- [50] X. Luo, J. Xu, B. Mohanty, and N. Xu, *J. Phys. G: Nucl. Part. Phys.* **40**, 105104 (2013).
- [51] M. Zhou and J. Jia, *Phys. Rev. C* **98**, 044903 (2018).
- [52] T. Sugiura, T. Nonaka, and S.I. Esumi, *Phys. Rev. C* **100**, 044904 (2019).
- [53] A. Chatterjee, Y. Zhang, J. Zeng, N. R. Sahoo, and X. Luo, *Phys. Rev. C* **101**, 034902 (2020).
- [54] A. Bzdak, V. Koch, and N. Strodthoff, *Phys. Rev. C* **95**, 054906 (2017).
- [55] A. Bzdak and V. Koch, *Phys. Rev. C* **96**, 054905 (2017).
- [56] M. Cheng *et al.*, *Phys. Rev. D* **79**, 074505 (2009).
- [57] X.-F. Luo (STAR Collaboration), *J. Phys.: Conf. Ser.* **316**, 012003 (2011).
- [58] X. Luo, *J. Phys. G: Nucl. Part. Phys.* **39**, 025008 (2012).
- [59] B. Ling and M. A. Stephanov, *Phys. Rev. C* **93**, 034915 (2016).
- [60] M. Kitazawa and X. Luo, *Phys. Rev. C* **96**, 024910 (2017).
- [61] A. Bzdak, V. Koch, and V. Skokov, *Eur. Phys. J. C* **77**, 288 (2017).
- [62] S. He and X. Luo, *Phys. Lett. B* **774**, 623 (2017).
- [63] M. Isse, A. Ohnishi, N. Otuka, P. K. Sahu, and Y. Nara, *Phys. Rev. C* **72**, 064908 (2005).
- [64] Y. Nara, N. Otuka, A. Ohnishi, K. Niita, and S. Chiba, *Phys. Rev. C* **61**, 024901 (1999).
- [65] Y. Nara, H. Niemi, A. Ohnishi, and H. Stöcker, *Phys. Rev. C* **94**, 034906 (2016).
- [66] Y. Nara, H. Niemi, J. Steinheimer, and H. Stöcker, *Phys. Lett. B* **769**, 543 (2017).
- [67] T. Hirano and Y. Nara, *Prog. Theor. Exp. Phys.* **2012**, 01A203.
- [68] H. Sorge, *Phys. Rev. Lett.* **82**, 2048 (1999).
- [69] S. He, X. Luo, Y. Nara, S. Esumi, and N. Xu, *Phys. Lett. B* **762**, 296 (2016).
- [70] Y. Ohnishi, M. Kitazawa, and M. Asakawa, *Phys. Rev. C* **94**, 044905 (2016).
- [71] J. Brewer, S. Mukherjee, K. Rajagopal, and Y. Yin, *Phys. Rev. C* **98**, 061901(R) (2018).